J. Astrophys. Astr. (2019) 40:29
https://doi.org/10.1007/s12036-019-9602-5

Temporal variations of the solar EUV network properties

BILIN SUSAN VARGHESE[1,*], K. P. RAJU[2] and P. J. KURIAN[1]

[1]Department of Physics, St. Berchmans College, Changanassery 686 101, India.
[2]Indian Institute of Astrophysics, Bengaluru 560 034, India.
*Corresponding author. E-mail: bilinsusan@gmail.com

MS received 15 April 2019; accepted 11 July 2019; published online 8 August 2019

Abstract. The chromospheric network extended to the transition region as the solar EUV network disperses at the coronal level. The EUV emission lines from the transition region give information about different atmospheric heights. The network properties have been obtained from the daily spectroscopic data from the Coronal Diagnostic Spectrometer (CDS) on board the Solar and Heliospheric Observatory (SOHO) in two lines He I 584.5 Å and O V 630 Å. The synoptic changes in the line intensity, skewness of intensity distribution, mean contrast and network index with respect to the sunspot cycle were studied for a period of 11 years from 1996 to 2006. We have obtained the cross correlation of the monthly average of these quantities with the monthly sunspot number. The mean intensity and skewness of the two lines generally show a positive correlation with the sunspot cycle. The network contrast and network index of the He I shows a definite negative correlation with the sunspot cycle. The negative correlations shown by the He I line are unexpected which could be due to its anomalous behaviour. There are differences in the behaviour of the two lines regarding the time lag with the sunspot cycle and the magnitude of the correlation which is always higher for the He I line. The results have implications to the studies of solar irradiance, magnetic flux transfer and solar atmospheric dynamics.

Keywords. Transition region—supergranulation—sunspots.

1. Introduction

The solar transition region is a narrow layer between the chromosphere and corona with a thickness of about 100 km. The density drops as we move through the solar atmosphere, and the temperature increases rapidly from 10^4 K to 10^6 K within the transition region. This sudden rise of atmospheric temperature remains as one of the major unresolved problems. To explain this increase of temperature, various mechanisms like wave heating, fine-scale magnetic flare heating, heating by chromospheric and coronal jets and spicules, etc. have been suggested (Walsh & Ireland 2003; Klimchuk 2006; De Pontieu *et al.* 2007; van Ballegooijen *et al.* 2011; McIntosh *et al.* 2011; Wedemeyer-Bohm *et al.* 2012; Parker 1988). It is generally accepted that the increase of thermal energy is due to the conversion of various wave and magnetic energies. Recent high-resolution observations made by SOHO, Transition Region and Coronal Explorer (TRACE), and *Hinode* indicate that the transition region is highly non-uniform and magnetically structured. Through a combination of spectroscopic monitoring and magnetic field calculations, the transition region was found to have different properties in different regions (Tian *et al.* 2010). The dynamic nature of the solar and stellar atmospheres can be known from the spectral line shifts and broadenings. Broadened line profiles are generally found in the transition region spectra of the solar atmosphere. A systematic study of the line broadenings and Doppler shifts performed using SUMER on SOHO is well explained by Chae *et al.* (1998) and Peter (2000). The nature of this broadening puts constraints on possible heating process. The transition region above sunspots was found to be higher and probably more extended (Tian *et al.* 2009).

SOHO, launched on 2 December 1995, has provided a continuous view of the Sun at many wavelengths. CDS on-board SOHO observes the solar spectrum and detects emission lines from ions and atoms in the chromosphere, transition region and corona. This gives information on the temperature, density and line shifts in the solar atmosphere. The synoptic studies are carried out by the Normal Incidence Spectrometer (NIS) of the CDS which takes data from two spectral windows.

The wavelength ranges of the two spectral windows are 308 (381 Å) and 513 (633 Å) (Harrison *et al.* 1995). Since the temperature of the Sun varies with the height, various emission lines give information of different atmospheric heights. The EUV emission covers a wavelength range from 100 to 1240 Å, comes from a temperature range of 8000 K to 4×10^6 K and can be used to obtain the physical properties of the solar atmosphere (Harrison *et al.* 1997).

The relation between the magnetic field and supergranules determines the structure of the transition region (Gabriel 1976). The convective motions in the Sun are seen at the surface as granules and supergranules. The network emission in the chromosphere and transition region arises from the convection motions within the supergranules which result in concentrations of magnetic field at their edges (Gallagher *et al.* 1998). The magnetic fields rise through the boundaries of supergranules and continuously change the upper solar atmosphere (Fuller-Rowell *et al.* 2004). Numerous studies were carried out on the intensity distribution of the quiet Sun in the solar atmosphere (Reeves 1976; Gallagher *et al.* 1998; Griffiths *et al.* 1999; Pauluhn *et al.* 2000; Fontenla *et al.* 1999). The quiet Sun intensity distributions have a skewed shape with a conspicuous peak at comparatively low intensities and a prolonged tail at higher intensities (Shakeri *et al.* 2015). From the Skylab observations in the 1970's, the resemblance of the EUV emission network with the Ca II chromospheric network is evident (Reeves *et al.* 1974).

An interesting feature of the transition region images is the strong intensity increase at the supergranule boundary in comparison with the cell interior (Reeves *et al.* 1974). For the EUV images formed in the chromospheric and transition region, the intensities above a value close to the mean can be identified with the bright network, and those below represent the cell interior (Gallagher *et al.* 1998). For the quiet Sun, Reeves (1976) found that the contrast between the network and the cell interior emission is largest for lines formed at 10^5 K and decreases at higher and lower temperatures. For the lines formed in the range 10^4 K to 10^5 K, approximately 85% of the observed intensity comes from 35% of the solar surface at the supergranular boundary (Reeves 1976). Curdt *et al.* (2008) explained the transition region redshift using the network contrast. According to Reeves (1976), for coronal lines the network contribution is only 50% of the total intensity, whereas for chromospheric and transition region lines, it is between 60 and 75% of the quiet Sun intensity. Schrijver *et al.* (1992) and Gallagher *et al.* (1998) found that the network coverage is about 50% in the Lyman line and in the emission lines of C II and O VI. Gallagher *et al.* (1998) reported that the contrast decreases with temperature from the He I to the He II lines, and then increases with temperature up to O V. Also the network is more well-defined in the transition region than in the chromosphere. The length scale of the network generally shows an increase from the chromosphere to the transition region (Gontikakis *et al.* 2003; Tian *et al.* 2008; Patsourakos *et al.* 1999).

This paper discusses the various properties of the EUV network in the solar transition region like the mean intensity, skewness of intensity distribution, network contrast and network index. Using the spectroscopic synoptic data from SOHO/CDS, the temporal changes of the network properties were examined for a period of 11 years during 1996–2006. The temporal variations of these properties are correlated with the solar cycle variations. As mentioned above, network is an important component which contributes to the solar irradiance. The two lines considered, He I 584.5 Å and O V 630 Å give us information about the two heights in the solar atmosphere. This will give some insight on the transition region heating and the corresponding energy transfer.

We obtain the following properties of the network:

(1) The mean intensity of the observational window.
(2) Skewness of the intensity distribution of the network which gives a measure of asymmetry. Skewness can be calculated using the equation

$$\text{Skewness } (S) = \frac{3(\text{mean} - \text{median})}{\text{standard deviation}}. \quad (1)$$

(3) Network contrast is the difference in brightness that makes the network distinguishable. Contrast can be defined using the standard expression

$$C = \frac{I_{\text{mean}}(\text{network}) - I_{\text{mean}}(\text{cell})}{I_{\text{mean}}(\text{network}) + I_{\text{mean}}(\text{cell})}, \quad (2)$$

where I_{mean}(network) is the mean intensity of the network and I_{mean}(cell) is the mean intensity of the cell interior.
(4) The network index or the normalised network area is defined as the number of pixels with a value above I_{min} divided by the total number of pixels within the image.

2. Data and analysis

The data were obtained from the CDS SYNOP observations (Harrison *et al.* 1995). All SYNOP versions included the He I and O V lines. The details of the observations and emission parameters are given in Tables 1

Table 1. Observation details.

Instrument	CDS/NIS
Slit	2×240 arcsec
Pixel resolution	2.03×1.68 arcsec
Exposure time	15 s
Wavelength range	1 Å

Table 2. Details of emission lines. The columns represent the ion, wavelength and the formation temperature respectively.

Ion	λ (Å)	$\log T/K$
He I	584	4.5
O V	630	5.4

and 2. The SYNOP data consisted of nine raster images over the solar meridian with each image having a size of 4×4 arcmin. Only the central image which is over the disk center was considered. The exposure time was 15 s and a raster image involved 120 steps which took about 42 min to complete. We have also considered only those images whose intensity lies within the two sigma level of the mean intensity of all images. This will avoid the images with active regions. Hence the observational window included the quiet-Sun and the coronal hole regions. If there was no quiet-Sun region near the disk center on a particular day, that data was omitted. In addition, there were several data gaps due to instrument problems, bad exposure, etc. The data covered a period of 11 years from 1996 to 2006 which involved about 2675 images. Analysis was done by using Solar SoftWare (SSW) in Interactive Data Language (IDL) environment. The data were first corrected to remove the effects of cosmic rays and then flat-fielded. Finally, they were calibrated to convert the photon count rates into absolute units, ($\mathrm{cm}^{-2}\ \mathrm{s}^{-1}\ \mathrm{arcsec}^{-1}$). Spectral purity of the images was ensured by selecting a wavelength range that included only the line of interest. We considered only those images whose intensity lies within the two sigma level of the mean intensity of all images. This helps avoid images with plages at the higher intensity level, and those with exposure problems at the lower intensity level.

The next step is to decide the network points. For this, we obtain the median-filtered image with a structural element of 15×15 pixels. The original image was then divided by the filtered image. The threshold intensity of the network, $I_{\min}$ was found by trial and error. The area and intensity of the network elements in each image was obtained by selecting those pixels with intensity above the chosen threshold. By trial and error, pixels with values above 1.14 (for He I window) and 1.16 (for O V window) in the resultant image were marked as network areas and below that the cell interior. The contrast is obtained from the mean values of the network and cell interior.

3. Results and discussion

Most of the EUV lines are known to show significant variation from solar minimum to solar maximum. Also, the intensity distributions for the network and the cell are significantly different in most of the lines below the coronal level (Raju 2010). We have first obtained the mean intensity of the window from the selected images. The aim is to see the solar cycle variation of the intensity which mostly originates from the network. The monthly sunspot number during the period 1996–2006 is given in Figure 1. The temporal variations of intensities of the lines are given in Figure 2. The individual measurements show a large scatter. The average intensity values obtained are 59 ± 20 units for the He I line and 23 ± 5 units for the O V line. The average intensity is given in units of photons $\mathrm{cm}^{-2}\ \mathrm{s}^{-1}\ \mathrm{arcsec}^{-1}$. The monthly average of the intensity values are also plotted in the figure which show a general positive correlation with the solar cycle. We have also obtained the cross correlation of these quantities with the monthly sunspot number which are also plotted. For the He line, the maximum correlation coefficient is 0.57 with evidence of lags at about 6 months and 1.5 years. The O line shows a reduced correlation coefficient of 0.23 with no clear

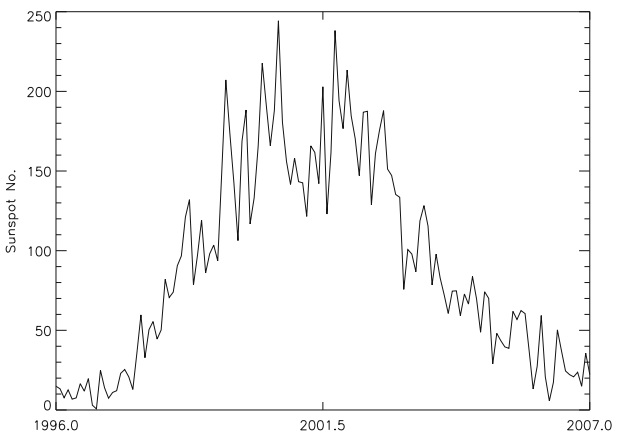

Figure 1. Variation of the monthly sunspot number during the period 1996–2006.

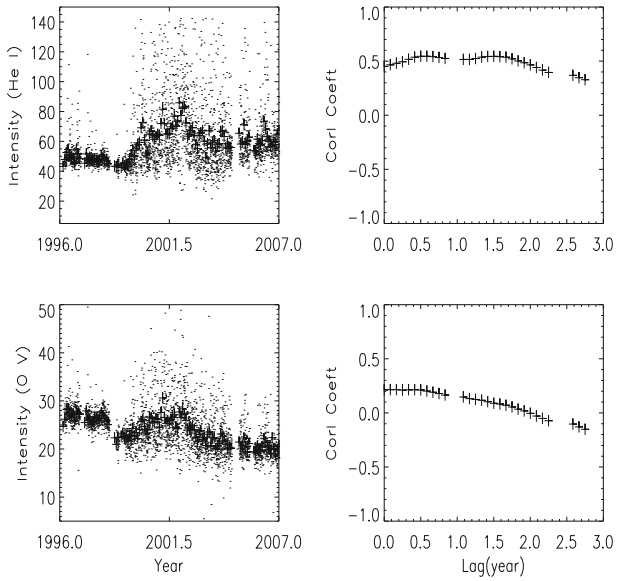

Figure 2. The left panels show the temporal variation of the intensity. The dots represent the individual measurements and pluses represent the monthly average. The right panels show the cross correlation of the monthly average with the sunspot number as a function of lag.

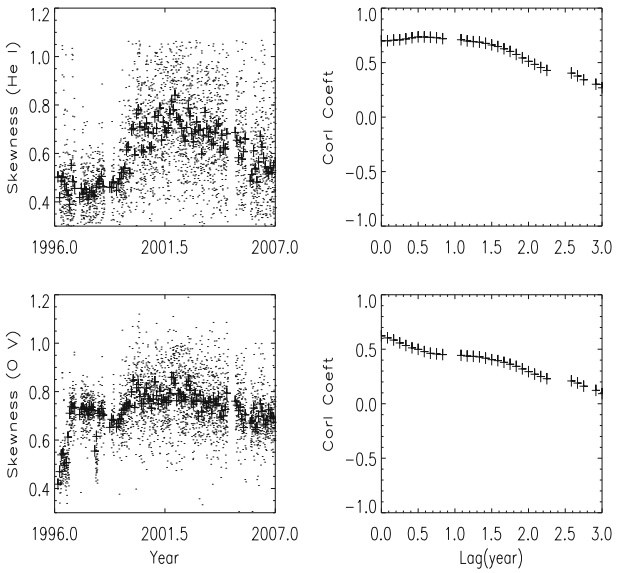

Figure 3. Temporal variation of the skewness of intensity distribution given in the left panels. The dots represent the individual measurements and pluses represent the monthly average. The right panels show the cross correlation of the monthly average with the sunspot number as a function of lag.

evidence of a lag. A few months of lag is generally expected between the sunspot number and the network properties as it may take some time for the dispersed flux to reach the network.

The temporal variation of skewness of intensity distribution is given in Figure 3. The average values of skewness obtained for the He I and O V lines are 0.60 ± 0.19 and 0.72 ± 0.13, respectively. The monthly average shows a clear positive correlation with the sunspot number for both the lines. The cross correlations of these quantities with the monthly sunspot number are obtained. The He line shows a maximum correlation coefficient of 0.75 with evidence of lag at about 6 months. For the O V line, the maximum correlation coefficient is 0.65 with no evidence of a lag. The skewed intensity distribution of the EUV lines is well-known from the Skylab days (Reeves *et al.* 1974). The high correlation of the skewness and sunspot cycle can be attributed to the availability of excess magnetic flux during solar maximum periods which contribute to the higher intensity tail of the distribution (Caccin *et al.* 1998; Raju & Singh 2002). It can also be seen that the average skewness is higher for the O V but the correlation with the solar cycle is more evident for the He I.

Next, we obtained the contrast between the network and cell interiors from the intensity images. The temporal variations of the network contrast are given in Figure 4. The average value of the network contrast

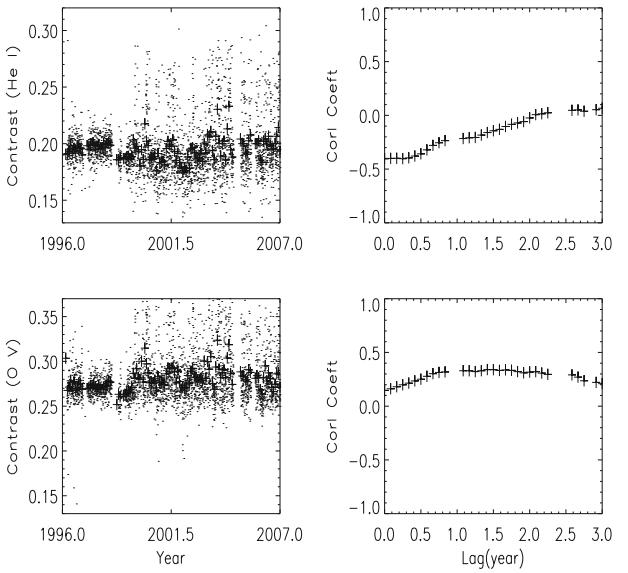

Figure 4. Temporal variations of the network contrast are given in the left panels. The dots represent the individual measurements and pluses represent the monthly average. The right panels show the cross correlation of the monthly average with the sunspot number as a function of lag.

for He I is 0.20 ± 0.02, and that for O V is 0.28 ± 0.03. According to Thompson (2006), Gallagher *et al.* (1998) and Raju (2010), the median contrast in the O V line is higher than that of the He I line which agrees with our

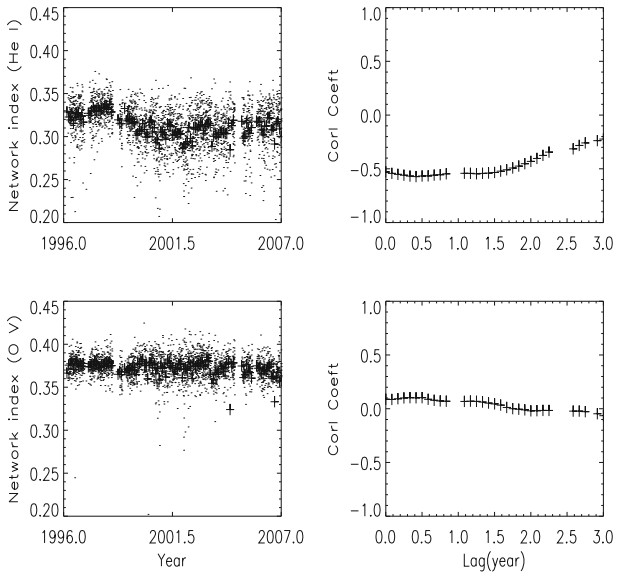

Figure 5. Temporal variations of the network index are given in the left panels. The dots represent the individual measurements and pluses represent the monthly average. The right panels show the cross correlation of the monthly average with the sunspot number as a function of lag.

result. This supports the well-known observation that the network is most prominent in the mid-transition region (Reeves 1976). The monthly averages show a complex picture as compared to the previous cases. The cross correlation with the monthly sunspot number given in the figure shows a negative correlation with a coefficient of −0.42 for the He I. The anti-correlation is rather surprising because the additional flux accumulated at the network boundaries during maximum periods is expected to enhance the contrast between the network and the interior. The enhanced network obtained from Ca II K chromospheric line show some evidence of increased contrast with the cycle (Worden *et al.* 2014). For the O V line, the correlation coefficient is 0.12 at zero lag which raises to 0.36 at a lag of ten months. The positive correlation is expected although the lag is somewhat surprising as it is not evident in the previous cases.

Finally, the network indices for the two lines were obtained from the images. The temporal variations of the network index are given in Figure 5. The average value of the network index for He I is 0.31 ± 0.03, and that for O V is 0.37 ± 0.02. These values are slightly greater than the value reported for the Ca II K line which is about 0.3 (Caccin *et al.* 1998; Singh *et al.* 2012). The higher value of O V again implies the prominence of the network in the transition region. The monthly averages of the network index show a negative correlation with the sunspot cycle for He I line and a lack of correlation for the O V line. The cross correlation with the monthly sunspot number plotted in the figure gives a correlation coefficient of −0.58 for the He I and 0.13 for the O V line. The observations of the chromospheric Ca II K line have reported a positive correlation between the network index and the sunspot cycle (Priyal *et al.* 2014; Raju & Singh 2014). So a similar positive correlation is expected in the case of the transition region lines, He I and O V. The prominent negative correlation in the case of He I is interesting and probably reported for the first time. The He lines are known to show anomalous behavior due to the resonance scattering mechanism of the line emission and large optical depth (Gallagher *et al.* 1998; Patsourakos *et al.* 1999; Jordan *et al.* 2001). The negative correlations of the network contrast and index with the sunspot cycle for the He I line are further examples of its anomalous behavior, and are probably related to each other. The O V line emission is dominated by the collisional excitation, while the He I line is contributed by both collisional and photo excitations. Through resonant scattering, He I emission is affected by the coronal emission which is different in the quiet-Sun and the coronal holes. This means that the network regions in the quiet-Sun are at a higher intensity level than that in the coronal hole region. Our observational window includes both quiet-Sun and coronal hole regions which could make the long-term variation of network properties somewhat complex. Detailed modelling is needed to fully understand the implications of the results.

Network is the main contributor to solar irradiance and they are also known as the source region of energetic phenomena like jets and spicules. Recent high-resolution IRIS observations have revealed that the two dominant contributors to the transition region emission are fast intermittent jets (Tian *et al.* 2014) and rapidly varying loops (Hansteen *et al.* 2014), both rooted in the transition region network. Hence studies of its properties and temporal variations are useful in modelling the solar atmospheric heating, energy transfer and irradiance. Although the He I line does not always show the transition region characteristics due to its anomalous behavior, the results in general show that the network properties vary with the solar cycle which can affect the energy budget of the loops and jets.

4. Conclusions

An extensive study of the network properties have been carried out using the SOHO/CDS SYNOP data for a

period of 11 years from 1996 to 2006 which almost covered the Solar Cycle 23. The physical characteristics of the solar EUV network like the mean intensity, skewness, contrast and the network index were obtained in the emission lines He I 584.5 Å and O V 630 Å. The temporal variations of these characteristics were compared with the sunspot cycle. It has been found that the mean intensity and skewness of the two lines show a positive correlation with the sunspot cycle. The average skewness is higher for O V but the correlation with the solar cycle is more prominent for He I. The two lines show different behaviour in terms of lag. The He I line shows some evidence of lags but no clear evidence of lag in the case of the O V line. The average value of the network contrast for He I is 0.20 ± 0.02, and that for O V is 0.28 ± 0.03. The cross correlation with the sunspot number shows a negative correlation for the He I and a positive correlation with a lag of ten months for the O V line. The average value of the network index for He I is 0.31 ± 0.03, and that for O V is 0.37 ± 0.02 which are slightly greater than the value reported for chromospheric Ca II K line. The monthly averages of the network index show a negative correlation with the sunspot cycle for He I line and a lack of correlation for the O V line. This is entirely different from the behaviour of the Ca II K line which shows a positive correlation between the network index and the sunspot cycle. The results generally support the fact that the network is most prominent in the mid-transition region. The negative correlations of the network contrast and the index with the sunspot cycle for the He I line are reported for the first time which need to be further probed by observational and modelling efforts.

Acknowledgements

The data was provided, courtesy: SOHO/EIT and CDS consortia. SOHO is a project of international cooperation between ESA and NASA. This work was funded by the Department of Science and Technology, Government of India.

References

Caccin B., Ermolli I., Fofi M., Sambuco A. M. 1998, Sol. Phys., 177, 295B
Chae J., Schuhle U., Lemaire P. 1998, ApJ, 505, 957C
Curdt W., Tian H., Dwivedi B. N., Marsh E. 2008, A&A, 491, 13C
De Pontieu B., McIntosh S. W., Carlsson M., Hansteen V. H., Tarbell T. D., Schrijver C. J., Title A. M., Shine R. A., Tsuneta S., Katsukawa Y., Ichimoto K., Suematsu Y., Shimizu T., Nagata S. 2007, Science, 318, 1574D
Fontenla J. M., Curdt W., Avrett E. H., Harder J. 1999, A&A, 468, 695F
Fuller-Rowell T., Solomon S., Roble R., Viereck R. 2004, Solar variability and its effects on climate, Geophys. Monograph, 141, 341F
Gabriel A. H. 1976, Philos. Trans. R. Soc. London, 281, 339G
Gallagher P. T., Phillips K. J. H., Harra-Murnion L. K., Keenan F. P. 1998, A&A, 335, 733G
Gontikakis C., Peter H., Dara H. C. 2003, A&A, 408, 743
Griffiths N. W., Fisher G. H., Woods D. T., Siegmund O. H. W. 1999, ApJ, 512, 992G
Hansteen V., De Pontieu B., Carlsson M., Lemen J., Title A., Boerner P., Hurl-burt N., Tarbell T. D., Wuelser J. P. *et al.* 2014, Science, 346, 1255757.
Harrison R. A., Sawyer E. C., Carter M. K., Cruise A. M., Cutler R. M., Fludra A. *et al.* 1995, Sol. Phys., 162, 233H
Harrison R. A., Fludra A., Pike C. D., Payne J., Thompson W. T., Poland A. I., Breeveld E. R., Culhane J. L., Kjeldseth-moe O., Huber M. C. E., Aschenbach B. 1997, Sol. Phys., 170, 123H
Jordan C., Macpherson K. P., Smith G. R. 2001, MNRAS, 328, 1098J
Klimchuk J. A. 2006, Sol. Phys., 234, 41K
McIntosh S. W., de Pontieu B., Carlsson M., Hansteen V., Boerner P., Goossens M. 2011, Nature, 475, 477M
Parker E. N. 1988, ApJ, 330, 474
Patsourakos S., Vial J. C., Gabriel A. H., Bellamine N. 1999, ApJ, 522, 540P
Pauluhn A., Solanki S. K., Rüedi I., Landi E., Schühle U. 2000, A&A, 362, 737P
Peter H. 2000, A&A, 360, 761
Priyal M., Singh J., Ravindra B., Priya T. G., Amareswari K. 2014, Sol. Phys. 289, 137P
Raju K. P., Singh J. 2002, Sol. Phys., 207, 11R
Raju K. P. 2010, Sol. Phys., 262, 61R
Raju K. P., Singh J. 2014, RAA, 14, 229
Reeves E. M., Foukal P. V., Huber M. C. E. 1974, ApJ, 188L, 27R
Reeves E. M. 1976, Sol. Phys., 46, 53R
Schrijver C. J., Zwaan C., Balke A. C., Tarbell T. D., Lawrence J. K. 1992, A&A, 253L, 1S
Shakeri F., Teriaca L., Solanki S. K. 2015, ApJ, 581A, 51S
Singh J., Belur R., Raju S., Pichaimani K., Priyal M., Gopalan Priya T., Kotikalapudi A. 2012, RAA, 12, 201S
Tian H., Marsch E., Tu C.-Y., Xia L.-D., He J.-S. 2008, A&A, 482, 267
Tian H., Curdt W., Teriaca L., Landi E., Marsch E. 2009, A&A, 505, 307
Tian H., Marsch E., Tu C.-Y., Curdt W., He J.-S. 2010, New Astron. Rev., 54, 13T

Tian H., DeLuca E. E., Cranmer S. R., De Pontieu B., Peter B., Martínez-Sykora J. *et al.* 2014, Science 346, 1255711

Thompson W. T. 2006, Eur. Space Agency Proc., 617E, 80T

van Ballegooijen A. A., Asgari-Targhi M., Cranmer S. R., DeLuca E. E. 2011 ApJ, 736, 3V

Walsh R. W., Ireland J. 2003, A&A Rev., 12, 1W

Wedemeyer-Bohm S., Scullion E., Steiner O., van der Voort L. R., de La Cruz Rodriguez J., Fedu V. 2012, Nature, 486, 505W

Worden J. R., White O. R., Woods T. N. 2014, ApJ, 496, 998